Communication

Revisiting Kekulene: Synthesis and Single Molecule Imaging

Iago Pozo, Zsolt Majzik, Niko Pavli#ek, Manuel Melle-Franco,
Enrique Guitián, Diego Peña, Leo Gross, and Dolores Pérez

Just Accepted

1
2
3
4
5
6
7
8
9
10
11
12
13
14
15
16
17
18
19
20
21
22
23
24
25
26
27
28
29
30
31
32
33
34
35
36
37
38
39
40
41
42
43
44
45
46
47
48
49
50
51
52
53
54
55
56
57
58
59
60

Revisiting Kekulene: Synthesis and Single Molecule Imaging

Iago Pozo[†], Zsolt Majzik[‡], Niko Pavliček[‡], Manuel Melle-Franco[§], Enrique Guitián[†], Diego Peña*[†], Leo Gross[‡] and Dolores Pérez*.

[†] Centro Singular de Investigación en Química Biolóxica e Materiais Moleculares (CIQUS) and Departamento de Química Orgánica, Universidade de Santiago de Compostela, 15782 Santiago de Compostela (Spain)

[‡] IBM Research – Zürich. 8803 Rüschlikon (Switzerland)

[§] CICECO, Aveiro Institute of Materials, Department of Chemistry. University of Aveiro. 3810-193 Aveiro (Portugal)

Supporting Information Placeholder

ABSTRACT: Four decades after the first (and only) reported synthesis of kekulene, this emblematic cycloarene has been obtained again through an improved route involving the construction of a key synthetic intermediate, 5,6,8,9-tetrahydrobenzo[*m*]tetraphene, by means of a double Diels-Alder reaction between styrene and a versatile benzodiyne synthon. Ultrahigh resolution AFM imaging of single molecules of kekulene and computational calculations provide additional support for a molecular structure with a significant degree of bond localization in accordance with the resonance structure predicted by Clar model.

Cycloarenes[1] constitute a fascinating class of polycyclic aromatic hydrocarbons (PAHs) that have attracted the scientific community for decades due to the singularity of their molecular and electronic structures.[2] They serve as ideal platforms to investigate fundamental questions around the concept of aromaticity and, in particular, those related with the π-electron distribution in complex aromatic systems.[3] Recently, renewed attention in cycloarenes has arisen since they serve as models for graphene pores.[4] Kekulene (**1**) is probably the best studied member of this family. Its electronic structure has been the subject of debate for decades,[5] being the Clar model **1a** and the annulenoid Kekule structure **1b** of special interest (Figure 1). In fact, properties such as superaromaticity[6,7] have been initially attributed to this molecule, associated to hypothetically representative annulenoid structures such as **1b**, comprising two concentric [4n+2] π-electron circuits.

While many theoretical studies on the electronic structure of cycloarenes have been reported, the experimental study of their properties has found limitations due to the extremely challenging synthesis of this kind of planar, *cata*-condensed aromatic macrocyclic systems.[2] In fact, the synthesis and characterization of kekulene by Staab and Diederich in

1978[1,8] is considered to be a landmark achievement in the field of aromatic chemistry. Only two additional nearly planar, unsubstituted cycloarenes, cyclo[*d,e,d,e,d,e,d,e,e*]deka-kisbenzene[9] and septulene[10] have been synthetized so far, while substituted analogues of kekulene and of the higher homologue, non-planar, octulene have been recently accessed taking advantage of their higher solubility.[11] However, the Staab & Diederich's synthesis of the parent kekulene (Scheme 1) remains unsurpassed, and apparently unrepeated, since the only available experimental studies on **1** are those reported by this group forty years ago.[1,8,12]
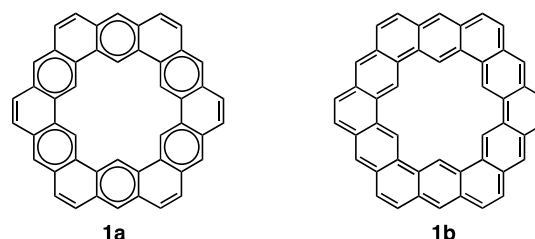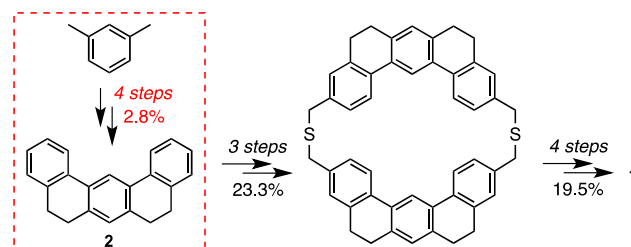

Figure 1. Clar (**1a**) and Kekule annulenoid (**1b**) structures of kekulene


Scheme 1. Synthetic approach to kekulene by Staab and Diederich[1,8a]

Our expertise and continuing interest in the chemistry of polycyclic aromatic compounds and nanographenes led us to turn our attention to this captivating molecule. Thus, here we present our contribution to the study of

kekulene through three different, yet related achievements: the improved synthesis of **1** by means of the aryne-mediated construction of a key synthetic intermediate, the single-molecule imaging of this fascinating cycloarene by ultrahigh resolution atomic force microscopy (AFM) and a computational study including the accurate simulation of the experimentally observed AFM images.

As shown in Scheme 1, probably the main drawback of the otherwise superb synthesis of **1** is the preparation of 5,6,8,9-tetrahydrobenzo[*m*]tetraphene (**2**).[13] The construction of the key synthetic intermediate **2**, far from being straightforward, was reported to occur in four steps, involving relatively harsh reaction conditions and in a poor overall 2.8% yield (Scheme 2a).[1] Our wide experience in the application of bistriflate **5** and other bisaryne precursors to the synthesis of diverse PAHs of interest,[14,15] led us to envision an alternative approach to **2** through a double Diels-Alder reaction involving two molecules of styrene (**3**) and the 1,4-benzodiyne synthon **4**, which would be generated by fluoride induced elimination from bistriflate **5**,[16] which is currently commercially available (Scheme 2b).
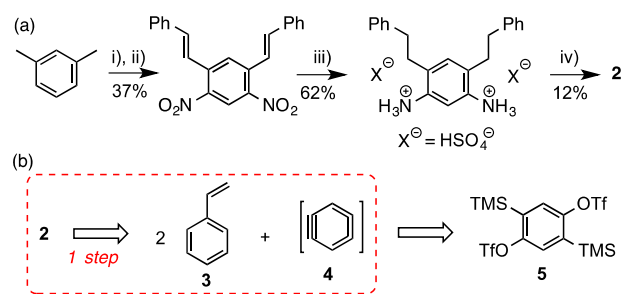
Scheme 2. (a) Staab&Diederich's synthesis of **2**:[1] i) conc. HNO₃, Δ; ii) PhCHO, piperidine; iii) H₂, 90 atm, 10%Pd/C, Δ; iv) Cu, conc. H₂SO₄, isoamyl nitrite. (b) This work: aryne-based retrosynthetic approach to **2**.

The participation of styrenes as unconventional dienes in Diels-Alder cycloadditions with arynes to yield dihydrophenanthrenes has been previously reported, although these transformations are commonly complicated by secondary reactions such as aryne-mediated dehydrogenation to give phenanthrenes,[17] or by the concerted ene reaction of the initial Diels-Alder adduct with a second aryne equivalent to afford arylated products.[18] In our case, such a Diels-Alder/ene cascade would be particularly problematic, since the ene-incorporated aryl moiety would contain *ortho*-disposed trimethylsilyl and triflate functionalities, being able to generate new aryne species and giving rise, probably, to oligomerization processes and complex reaction mixtures. Despite these possible difficulties, we targeted the synthesis of **2** by reaction of styrene with 1,4-bisbenzyne precursor **5** under aryne-forming conditions (Scheme 3, Table 1).

Initial essays were performed in refluxing dioxane using CsF as the fluoride source, conditions that had been previously reported for the unusual selective preparation of non-arylated 9,10-dihydrophenanthrene by reaction of styrene with benzyne.[19] Encouragingly, treatment of **5** with CsF in refluxing dioxane, in the presence of excess **3**, resulted in the formation of the expected products **2** and **6**, although in modest yield (entry 1). Addition of 18-crown-6 (entry 2) or the use of TBAF as fluoride source (entry 3) led to poorer results.
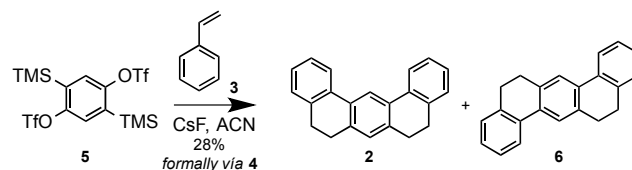
Scheme 3. Reaction of bistriflate **5** with CsF in presence of styrene

Table 1. Optimization of the reaction conditions[a]

Entry	Solvent	Molar ratio 5:3:CsF	Scale (mmol 5)	Yield 2+6 (%)[b]
1	Dioxane	1:5:10	0.2	17
2[c]	Dioxane	1:5:10	0.2	11
3[d]	Dioxane	1:5:10	0.2	–
4[e]	ACN	1:5:10	0.2	13
5	ACN	1:5:10	0.2	20
6	ACN	1:2:10	0.2	12
7[f]	ACN	1:25:10	0.2	23
8	ACN	1:5:6	0.2	20
9	ACN	1:5:6	1.4	22
10	ACN	1:5:6	6	26
11	ACN	1:5:6	19	28

[a]Typical reaction conditions: reflux under Ar, 16 h, [**5**] = 0.05 M. [b]Yield of isolated product (≈ 2:3 mixture of **2** and **6**). [c]18-crown-6 (120 mol%) was added. [d]TBAF was used as source of fluoride. [e]Reaction conducted at room temperature. [f][**5**] = 0.01 M.

The use of acetonitrile (ACN) as solvent led to slightly better yields (entry 5) and, in these conditions, the molar ratio **5**:**3**:CsF was optimized (entries 5-8). Finally, we proved that better yields were consistently obtained when performing the reaction at higher scale (entries 8-11). The best results were obtained by reaction of **5** (19-20 mmol) with styrene (**3**) and CsF (in 1:5:6 molar ratio) in refluxing acetonitrile, yielding a 2:3 mixture of tetrahydrobenzotetraphenes **2** and **6** in a reasonable 28% yield (entry 11). The separation of both isomers was not easy, but it could be achieved by semi-preparative supercritical fluid chromatography (SFC)[20] and also by sequential recrystallizations from boiling methanol.

These results can be considered highly remarkable, since compound **2**, a key intermediate in the synthesis of kekulene (**1**), is obtained in just one step from

commercially available materials, under mild reaction conditions and with a fourfold increased yield with respect to that of the previously reported synthesis.
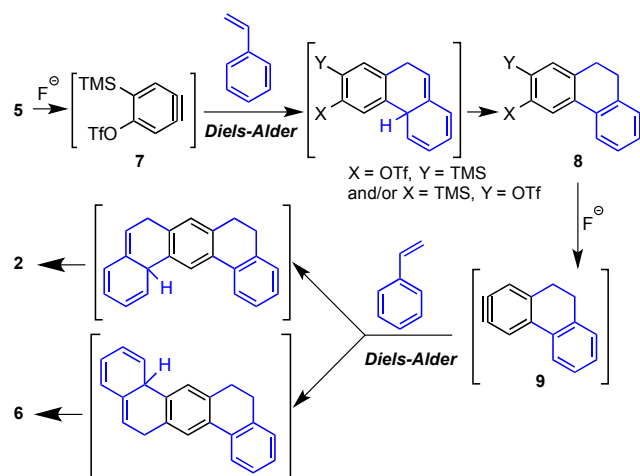
Scheme 4. Mechanistic proposal for the formation of **2/6**

Remarkably, the only isolable compounds detected in the crude reaction mixtures were **2**, **6** and excess styrene (**3**).[20] Products derived either from dehydrogenation of **2/6** or from Diels−Alder/ene cascade processes were not observed.[21] However, the formation of insoluble oligomers or polymers derived from aryne-based side reactions cannot be ruled out. The mechanism proposed for the formation of **2** (and **6**), involves two probably sequential Diels-Alder/H-migration processes. The detection of the functionalized dihydrophenanthrene **8** in some experiments, strongly suggests that the first Diels-Alder reaction of styrene with monoaryne **7** and the subsequent H-migration, occur prior to the generation of the second *arynic* insaturation in **9** (Scheme 4). Once compound **2** was conveniently prepared, we proceeded to complete the synthesis of kekulene (**1**). After attempting some new synthetic alternatives based on metal-catalyzed couplings and/or olefin metathesis/isomerization reactions, we decided to rely on the firmly established route described by Diederich and Staab,[1,8] which in our hands was perfectly reproducible, even under significantly lower scale conditions.
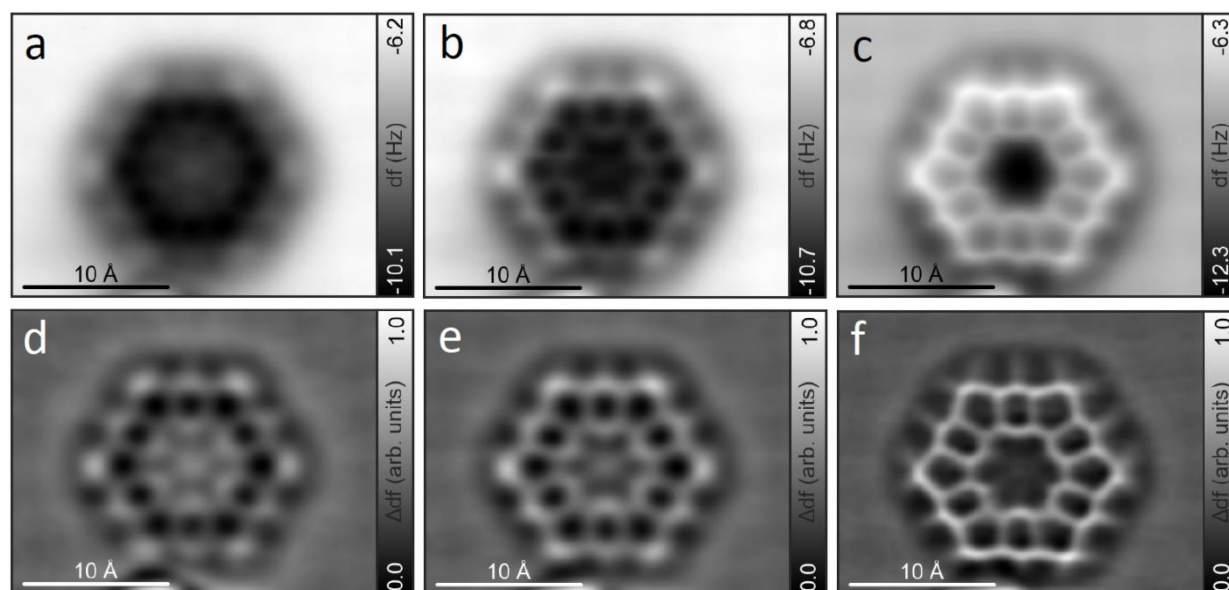
Figure 2. Experimental AFM images of kekulene (**1**) on Cu(111). (a-c) Constant-height AFM images with a CO functionalized tip, amplitude $A = 1$ Å, sample voltage $V = 0$ V. We approached the tip by $z = 1.6$ Å in (a), 1.9 Å in (b) and 2.2 Å in (c) with respect to the STM setpoint of $V = 0.1$ V, $I = 1$ pA on the bare Cu(111) surface. (d-e) Corresponding Laplace-filtered images.

With kekulene (**1**) in hand we identified the opportunity to visualize its molecular structure by ultrahigh resolution AFM,[22] a state-of-the-art technique for the single-molecule study of planar, conjugated systems. As recently demonstrated this technique, in combination with STM, has become a powerful tool for the elucidation and study of individual molecules.[23] In order to increase the sublimation rate with respect to the

fragmentation rate the material was sublimated by rapid heating[24a] from a Si wafer,[24b] onto a Cu(111) substrate, holding the sample at $T = 10$ K during deposition. The large size and thus high sublimation temperature of kekulene was expected to result in fragmentation and, in fact, the preparation resulted mostly in small and often mobile molecules on the surface. However, we found a few molecules of the expected hexagonal shape and size

of kekulene. Constant-height AFM images of the molecule adsorbed on Cu(111) with a CO functionalized tip[22,25-28] were recorded at different heights (Figure 2) with decreasing tip to sample distance from Fig. 2a to 2c. Corresponding Laplace filtered images are shown in Fig. 2d to 2f, respectively. From the AFM images, the molecular structure of kekulene (**1**) was resolved. In addition, details of the contrast can be related to bond order. Resolving the bond-order related contrast is challenging at the periphery of molecules because of the non-planar background from van der Waals and electrostatic forces.[27,29] However, bonds that experience similar background forces are comparable, allowing

qualitative resolution of bond-order differences. Increased bond order results in brighter appearance at moderate tip heights and shortened appearance of bonds at small tip heights.[27] In the case of kekulene (**1**), the peripheral C(H)–C(H) bonds appear as the overall brightest bonds at moderate tip height, i.e., in Fig. 2a,b, and as the shortest bonds at small tip height, i.e., in Fig. 2c. Both observations indicate that these are the bonds of the highest bond order within the kekulene structure, which is in agreement with previous experimental evidence obtained by X-ray diffraction (XRD) studies of single crystals of **1**.[8b]
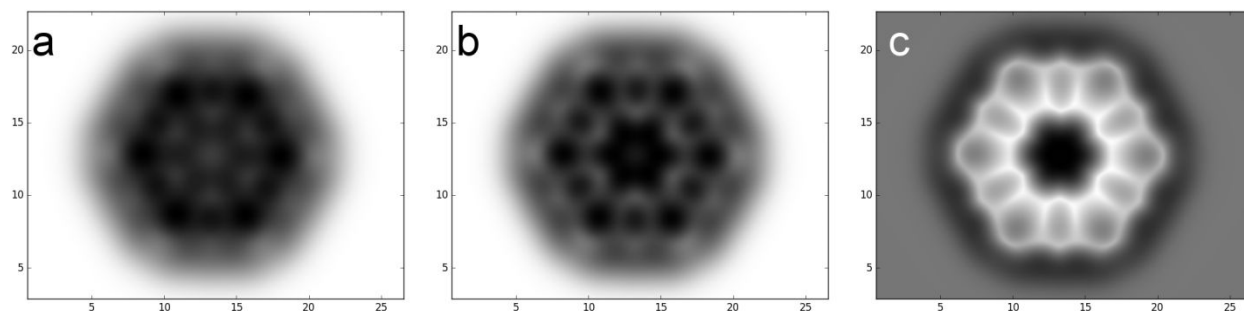
Figure 3. PPM simulated AFM images with an amplitude of A = 1 Å computed with a PBE QM/MM electrostatic potential interacting with a classical d_{z^2}-like quadrupole tip (Qd_{z^2}=-0.25 e$^-$ Å^{-2}) with a bending stiffness of 0.35 N/m at z= 3.4 Å in (a), 3.3 Å in (b) and 3 Å in (c) with respect to the molecular plane. All distances are in Å.

To gain further insight into the interpretation of the AFM images in connection with the molecular structure of **1**, we computed the kekulene molecule both in the gas phase and on the Cu(111) surface and performed simulations of AFM images.[20] Calculations in the gas-phase at the B3LYP-def2-TZVP level[30] reveal that the molecule possesses D_{3d} symmetry since the hydrogen atoms of the inner cavity or pore present a slight distortion out of the molecular plane due to steric hindrance. Remarkably, the calculated C–C bond distances reproduce the experimental solid-state XRD values within 0.01 Å (Figure 4). This bonding pattern, which is also reproduced by on-surface calculations, matches perfectly the predictions of the π-sextet rule[31] and supports the Clar model **1a**, with the highest possible number of disjoint aromatic π-sextets (six) as the most representative structure of kekulene. Thus, despite its 48 π electrons (6n π electrons) kekulene is far from being "fully benzenoid", as the π electrons are not highly delocalized. In fact, **1** possesses an unusually high calculated HOMO-LUMO gap of 3.55 eV (B3LYP-def2-TZVP level), similar to that calculated for the much smaller anthracene molecule (3.56 eV). Finally, simulations of the AFM images were performed with a Molecular Mechanics (MM) model as implemented in the Probe Particle Model (PPM) software.[20,28,32] We computed images with the experimental amplitude of 1.0 Å and with different bending constants, k, ranging from 0.15 to 0.60 N/m, and uncharged, monopole and quadrupole tips. The best

match to the experimental images was achieved by a d_{z^2}-like quadrupole tip[33] with Qd_{z^2} = -0.25 e$^-$/A^2 and a bending constant of k = 0.35 N/m, see Figure 3.[34]
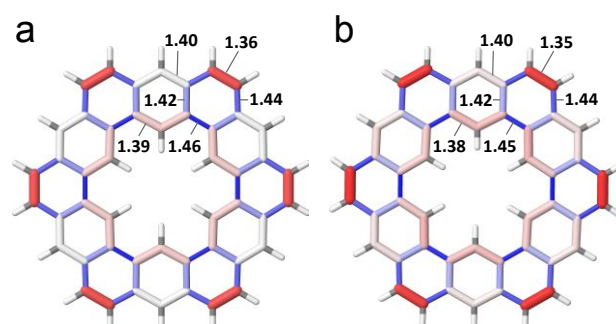
Figure 4. (a) Molecular structure of kekulene (**1**) computed at the B3LYP-def2-TZVP level in vacuum. (b) Experimental structure from XRD, C2/c space group symmetry. The colors grade with distance from 1.33 Å (red) to 1.40 Å (white) and to 1.47 Å (blue). Bond lengths are in Å.

In conclusion, this work provides a significant contribution to the synthesis of kekulene (**1**) based on the improved preparation of the key intermediate 5,6,8,9-tetrahydrobenzo[*m*]tetraphene (**2**) by means of aryne chemistry. The modified protocol has been applied to the actual synthesis of **1**, which, to the best of our knowledge, had not been synthesized neither

experimentally studied since the seminal work by Staab and Diederich in the early eighties. With this material in hand, the structure of individual molecules of kekulene (**1**) was nicely resolved by ultrahigh resolution AFM. The computational study of kekulene (**1**) in vacuum and on the Cu(111) surface and the successful simulation of the experimental single-molecule AFM images, provided further evidences of a bonding pattern for kekulene which matches with the molecular structure predicted by Clar's π-sextet rule.

ASSOCIATED CONTENT

The Supporting Information is available free of charge on the ACS Publications website. Experimental procedures, synthesis, characterization, AFM imaging and computational details (PDF).

AUTHOR INFORMATION

Corresponding Author

dolores.perez@usc.es
diego.pena@usc.es

ACKNOWLEDGMENT

REFERENCES

(1) Staab, H. A.; Diederich, F. Synthesis of Kekulene. *Chem. Ber.* **1983**, *116*, 3487−3503.

(2) For an excellent recent review, see: Buttrick, J. C.; King, B. T. Kekulenes, Cycloarenes, and Heterocycloarenes: Addressing Electronic Structure and Aromaticity through Experiments and Calculations. *Chem. Soc. Rev.* **2017**, *46*, 7−20.

(3) (a) Aihara, J. π-Electron Currents Induced in Polycyclic Benzenoid Hydrocarbons and their Relationship to Clar Structures. *J. Phys. Chem. A* **2003**, *107,* 11553-11557. (b) Randic, M. Aromaticity of Polycyclic Conjugated Hydrocarbons *Chem. Rev.* **2003**, *103*, 3449−3605. (c) Aihara, J.; Makin, M. Constrained Clar Formulas of Coronoid Hydrocarbons. *J. Phys. Chem. A* **2014**, *118*, 1258−1266. (d) Stepien, M. An Aromatic Riddle: Decoupling Annulene Conjugation in Coronoid Macrocycles. *Chem* **2018**, *4*, 1481-1491. (e) Liu, C.; Ni, Y.; Lu, X.; Li, G.; Wu, J. Global Aromaticity in Macrocyclic Polyradicaloids: Hückel's Rule or Baird's Rule? *Acc. Chem. Res.* **2019**, *52*, 2309-2321.

(4) (a) Robertson, A. W.; Lee, G.-D.; He, K.; Gong, C.; Chen, Q.; Yoon, E.; Kirkland, A. I.; Warner, J. H. Atomic Structure of Graphene Subnanometer Pores. *ACS Nano,* **2015**, *9*, 11599–11607. (b) Beser, U.; Kastler, M.; Maghsoumi, A.; Wagner, M.; Castiglioni, C.; Tommasini, M.; Narita, A.; Feng X.; Müllen, K. A C216-Nanographene Molecule with Defined Cavity as Extended Coronoid. *J. Am. Chem. Soc.* **2016**, *138*, 4322–4325. (c) Hieulle, J.; Carbonell-Sanromà, E.; Vilas-Varela, M.; García-Lekue, A.; Guitián, E.; Peña, D.; Pascual, J. I. On-surface Route for Producing Planar Nanographenes with Azulene Moieties. *Nano Lett.* **2018**, *18*, 418-423. (d) Moreno, C.; Vilas-Varela, M.; Kretz, B.; García-Lekue, A.; Costache, M. V.; Paradinas, M.; Panighel, M.; Ceballos, G.; Valenzuela, S. O.; Peña, D.; Mugarza, A. Bottom-up Synthesis of Multifunctional Nanoporous Graphene *Science* **2018**, *360*, 199-203. (e) Xu, K.; Urgel, J. I.; Eimre, K.; Giovannantonio, M. D.; Keerthi, A.; Komber, H.; Wang, S.; Narita, A.; Berger, R.; Ruffieux, P.; Pignedoli, C. A.; Liu, J.; Müllen, K.; Fasel, R.; Feng, X. On-Surface Synthesis of a Nonplanar Porous Nanographene. *J. Am. Chem. Soc.* **2019,** *141*, 7726-7730.

(5) For seminal contributions see: (a) McWeeny, R. The Diamagnetic Anisotropy of Large Aromatic Systems: III Structures with Hexagonal Symmetry. *J. Phys. Chem. A* **1951**, 921-930. (b) Aihara, J. On the Number of Aromatic Sextets in a Benzenoid Hydrocarbon. *Bull. Chem. Soc. Jpn.* **1976**, *49*, 1429–14230.

(6) (a) Cioslowski, J.; O'Connor, P. B.; Fleischmann, E. D. Is Superbenzene Superaromatic? *J. Am. Chem. Soc.* **1991**, *113*, 1086-1089. (b) Aihara, J. Is Superaromaticity a Fact or an Artifact? The Kekulene Problem. *J. Am. Chem. Soc.* **1992**, *114*, 865–868. (c) Jiao, H.; Schleyer, P. R. Is Kekulene Really Superaromatic?. *Angew. Chem. Int. Ed. Engl.* **1996**, *35*, 2383–2386. (d) Zhou, Z. Are kekulene, coronene, and corannulene tetraanion superaromatic? Theoretical examination using hardness indices. *J. Phys. Org. Chem.* **1995**, *8*, 103–107. (e) Aihara, J.; Makino, M.; Ishida, T.; Dias, J. R. Analytical Study of Superaromaticity in Cycloarenes and Related Coronoid Hydrocarbons. *J. Phys. Chem. A* **2013**, *117*, 4688–4697.

(7) The synthesis of two structurally related macrocyclic polyradicaloids, with "annulene-within-an-annulene" structure and unusual global aromaticity, has been recently reported: Liu, C.; Sandoval-Salinas, M. E.; Hong, Y.; Gopalaskrishna, T. Y.; Phan, H.; Aratani, N.; Herng, T. S.; Ding, J.; Yamada, H.; Kim, D.; Casanova, D.; Wu, J. Macrocyclic Polyradicaloids with Unusual Super-ring Structure and Global Aromaticity. *Chem* **2018**, *4*, 1–10.

(8) (a) Diederich, F.; Staab, H. A. Benzenoid versus Annulenoid Aromaticity : Synthesis and Properties of Kekulene. *Angew. Chem. Int. Ed. Engl.* **1978**, *17*, 372–374. (b) Krieger, C. Diederich, F.; Schweitzer, D. Staab, H. A. Molecular Structure and Spectroscopic Properties of Kekulene. *Angew. Chem. Int Ed. Engl.* **1979**, *18*, 669-701. (c) Staab, H. A.; Diederich, F.; Krieger, C.; Schweitzer, D. Molecular Structure and Spectroscopic Properties of Kekulene. *Chem. Ber.* **1983**, *116*, 3504–3512.

(9) Funhoff, D. J. H.; Staab, H. A. Cyclo[*d.e.d.e.e.d.e.d.e.e.*]decakisbenzene, a New Cycloarene. *Angew. Chem. Int. Ed. Engl.* **1986**, *25*, 742–744.

(10) Kumar, B.; Viboh, R. L.; Bonifacio, M. C.; Thompson, W. B.; Buttrick, J. C.; Westlake, B. C.; Kim, M.-S.; Zoellner, R. W.; Varganov, S. A.; Mörschel, P.; Teteruk, J.; Schmidt, M. U.; King, B. T. Septulene: The Heptagonal Homologue of Kekulene. *Angew. Chem. Int. Ed.* **2012**, *51*, 12795–12800.

(11) Majewski, M. A.; Hong, Y.; Lis, T.; Gregolinski, J.; Chmielewski, P. J.; Cybinska, J.; Kim, D.; Stepien, M. Octulene: A Hyperbolic Molecular Belt that Binds Chloride Anions. *Angew. Chem. Int. Ed.* **2016**, *55*, 14072–14076.

(12) Schweitzer, D.; Hausser, K. H.; Vogler, H.; Diederich, F.; Staab, H. A. Electronic Properties of Kekulene. *Mol. Phys.* **1982**, *46*, 1141–1153.

(13) This specific, partially hydrogenated PAH, is needed to guarantee the conformational flexibility required for the penultimate step in the synthesis of kekulene (a double photochemical cycloisomerization; see ref. 1 for details).

(14) (a) Schuler, B.; Collazos, S.; Gross, L.; Meyer, G.; Pérez, D.; Guitián, E.; Peña, D. From Perylene to a 22-Ring Aromatic Hydrocarbon in One-Pot. *Angew. Chem. Int. Ed.* **2014**, *53*, 9004–9006. (b) Rodríguez-Lojo, D.; Peña, D.; Pérez, D.; Guitián, E. Large Phenyl-Substituted Acenes by Cycloaddition Reactions of the 2,6-Naphthodiyne Synthon *Chem. Commun.* **2015**, *51*, 5418–5420. (c) Rodríguez-Lojo, D.; Peña, D.; Pérez, D.; Guitián, E. Straightforward Synthesis of Novel Acene-Based Aryne Precursors, *Synlett* **2015**, *26*, 1633–1637. (d) Pozo, I.; Cobas, A.; Peña, D.; Guitián, E.; Pérez, D. 1,7-Naphthodiyne: a New Platform for the Synthesis of Novel, Sterically Congested PAHs *Chem. Commun.* **2016**, *52*, 5534–5537. (e) Garcia, D., Rodríguez-Pérez, L.; Herranz, M. A.; Peña, D.; Guitián, E.; Bailey, S.; Al-Galiby, Q.; Noori, M.; Lambert, C. J.; Perez, D.; Martín, N. A C60-Aryne Building Block: Synthesis of a Hybrid All-Carbon Nanostructure. *Chem. Commun.* **2016**, *52*, 6677–6680. (f) Krüger, J.; García, F.; Eisenhut, F.; Skidin, D.; Alonso, J. M.; Guitián, E.; Pérez, D.; Cuniberti, G.; Moresco, F.; Peña, D. Decacene: On-Surface Generation *Angew. Chem. Int. Ed.*, **2017**, *56*, 11945–11948. (g) Schulz, F.; García, F.; Kaiser, K.; Pérez, D.; Guitián, E.; Gross, L.; Peña, D. Exploring a Route to Cyclic Acenes by On-Surface Synthesis. *Angew. Chem. Int. Ed.*, **2019**, *58*, 9038-9042.

(15) For representative examples by other authors, see: (a) Li, J.; Zhao, Y.; Lu, J.; Li, G.; Zhang, J.; Zhao, Y.; Sun, X.; Zhang, Q. Double [4+2] Cycloaddition Reaction to Approach a Large Acene with Even-Number Linearly Fused Benzene Rings: 6,9,16,19-Tetraphenyl-1.20,4.5,10.11,14.15-Tetrabenzooctatwistacene. *J. Org. Chem.* **2015**, *80*, 109–113. (b) Kumarasinhe, K. G. U. R.; Fronczek, F. R.; Valle, H. U.; Sygula, A. Bis-corranuleno-anthracene: An Angularly Fused Pentacene as a Precursor for Barrelene-Tethered Receptors for Fullerene. *Org. Lett.* **2016**, *18*, 3054–3057.

(16) Duong, H. M.; Bendikov, M.; Steiger, D.; Zhang, Q.; Sonmez, G.; Yamada, J.; Wudl, F. Efficient Synthesis of a Novel, Twistedand Stable, Electroluminescent "Twistacene". *Org. Lett.* **2003**, *5*, 4433–4436.

(17) (a) Wolthuis, E.; Cady, W. Reaction of Benzyne with α-Methylstyrene *Angew. Chem. Int. Ed.*, **1967**, *6*, 555–556. (b) Harrison, R.; Heaney, H.; Jablonski, J. M.; Mason, K. G.; Sketchley, J. M. Aryne Chemistry. Part XVIII. Some Reactions of Tetrahalogenobenzyneswith Styrene and Substituted Styrenes *J. Chem. Soc. C*, **1969**, 1684–1689.

(18) (a) Dilling, W. L. The Reaction of Benzyne with Styrene *Tetrahedron Lett.* **1966**, *9*, 939–941. (b) Bhojgude, S. S.; Bhunia, A.; Gonnade, R. G.; Biju, A. T. Efficient Synthesis of 9–Aryldihydrophenanthrenes by a Cascade Reaction Involving Arynes and Styrenes, *Org. Lett.* **2014**, *16*, 676–679. (c) Bhojgude, S. S.; Bhunia, A.; Biju, A. T. Employing Arynes in Diels-Alder Reactions and Transition-Metal-Free Multicomponent Coupling and Arylation Reactions *Acc. Chem. Res.* **2016**, *49*, 1658-1670.

(19) Chen, Z.; Han, X.; Liang, J. H.; Yin, J.; Yu, G. A.; Liu, S. H. Cycloaddition Reactions of Benzyne with Olefins. *Chinese Chem. Lett.* **2014**, *25*, 1535–1539.

(20) See Supporting Information for details.

(21) In some experiments performed in large scale, trace amounts of a monophenylated product were detected by mass spectrometry.

(22) Gross, L.; Mohn, F.; Moll, N.; Liljeroth, P.; Meyer, G. The Chemical Structure of a Molecule Resolved by Atomic Force Microscopy. *Science* **2009**, *325*, 1110–1114.

(23) (a) Gross, L.; Mohn, F.; Moll, N.; Liljeroth, P.; Meyer, G. Atomic Force Microscopy for Molecular Structure Ellucidation. *Angew. Chem. Int. Ed.* **2018**, *57*, 3888–3908 and references cited therein; (b) Peña, D.; Pavlicek, N.; Schuler, B.; Moll, N.; Pérez, D.; Guitián, E.; Meyer, G.; Gross L. in *On-Surface Synthesis II. Advances in Atom and Single Molecule Machines* (Eds.: D. de Oteyza, C. Rogero), Springer, Cham, **2018**, pp. 209-227. (c) Fatayer, S.; Albrecht, F.; Zhang, Y.; Urbonas, D.; Peña, D.; Noll, N.; Gross, L. Molecular structure elucidation with charge-state control. *Science* **2019**, *365*, 142-145. (d) de Oteyza, D. G.; Gorman, P.; Chen, Y.-C.; Wickenburg, S.;

Riss, A.; Mowbray, D. J.; Etkin, G.; Pedramrazi, Z.; Tsai, H.-Z.; Rubio, A.; Crommie, M. F.; Fischer, F. R. Direct Imaging of Covalent Bond Structure in Single-Molecule Chemical Reactions. *Science* **2013**, *340*, 1434-1437. (e) Rogers, C.; Chen, C.; Pedramrazi, Z.; Omrani, A. A.; Tsai, H.-Z.; Jung, H. S.; Lin, S.; Crommie, M. F.; Fischer, F. R. Closing the Nanographene Gap: Surface-Assisted Synthesis of Peripentacene from 6,6'-Bipentacene Precursors. *Angew. Chem. Int. Ed.* **2015**, *54*, 15143-15146. (f) Kawai, S.; Haapasilta, V.; Lindner, B. D.; Tahara, K.; Spijker, P.; Buitendijk, J. A.; Pawlak, R.; Meier, T.; Tobe, Y.; Foster, A. S.; Meyer, E. Thermal Control of Sequential On-Surface Transformation of a Hydrocarbon Molecule on a Copper Surface. *Nature Commun.* **2016**, *7*, 12711. (g) Hieulle, J.; Carbonell-Sanromà, E.; Vilas-Varela, M.; García-Lekue, A.; Guitián, E.; Peña, D.; Pascual, J. I. On-Surface Route for Producing Planar Nanographenes with Azulene Moieties. *Nano Lett.* **2018**, *18*, 418-423. (h) Fan, Q.; Werner, S.; Tschakert, J.; Ebeling, D.; Schirmeisen, A.; Hilt, G.; Hieringer, W. Gottfried, W. Precise Monoselective Aromatic C–H Bond Activation by Chemisorption of Meta-Aryne on a Metal Surface. *J. Am. Chem. Soc.* **2018**, *140*, 7526-7532. (i) Mishra, S.; Beyer, D.; Eimre, K.; Liu, J.; Berger, R.; Gröning, O.; Pignedoli, C. A.; Müllen, K.; Fasel, R.; Feng, X.; Ruffieux, P. Synthesis and Characterization of π-Extended Triangulene. *J. Am. Chem. Soc.* **2019**, *141*, 10621-10625. (j) Su, J.; Telychko, M.; Hu, P.; Macam, G.; Mutombo, P.; Zhang, H.; Bao, Y.; Cheng, F.; Huang, Z.-Q.; Qiu, Z.; Tan, S. J. R.; Lin, H.; Jelínek, P.; Chuang, F.-C.; Wu, J.; Lu, J. Atomically Precise Bottom-up Synthesis of π-Extended [5]Triangulene. *Sci. Adv.* **2019**, *5*, eaav7717. (k) Sánchez-Grande, A.; de la Torre, B.; Santos, J.; Cirera, B.; Lauwaet, K.; Chutora, T.; Edalatmanesh, S.; Mutombo, P.; Rosen, J.; Zbořil, R.; Miranda, R.; Björk, J.; Jelínek, P.; Martín, N.; Écija, D. On-Surface Synthesis of Ethynylene-Bridged Anthracene Polymers. *Angew. Chem. Int. Ed.* **2019**, *58*, 6559-6563.

(24) (a) Rapenne, G., Grill, L., Zambelli, T., Stojkovic, S.M., Ample, F., Moresco, F. and Joachim, C. Launching and landing single molecular wheelbarrows on a Cu (100) surface. *Chem. Phys. Lett.* **2006**, *431*, 219-222. (b) Schuler, B.; Meyer, G.; Peña, D.; Mullins, O. C.; Gross, L. Unraveling the Molecular Structures of Asphaltenes by Atomic Force Microscopy *J. Am. Chem. Soc.* **2015**, *137*, 9870–9876.

(25) Gross, L.; Mohn, F.; Moll, N.; Meyer, G.; Ebel, R.; Abdel-Mageed, W. M.; Jaspars, M. Organic Structure Determination Using Atomic Resolution Scanning Probe Microscopy. *Nat. Chem.* **2010**, *2*, 821–825.

(26) Bartels, L.; Meyer, G.; Rieder, K. H. Controlled Vertical Manipulation of Single CO molecules with the Scanning Tunneling Microscope: A Route to Chemical Contrast *Appl. Phys. Lett.* **1997**, *71*, 213–215.

(27) Gross, L.; Mohn, F. Moll, N.; Schuler, B.; Criado, A.; Guitián, E.; Peña, D. A. Gourdon, G. Meyer. Bond-Order Discrimination by Atomic Force Microscopy. *Science*, **2012**, *337*, 1326-1329.

(28) Hapala, P.; Kichin, G.; Wagner, C.; Tautz, F. S.; Temirov, R.; Jelínek, P. Mechanism of High-Resolution STM/AFM Imaging with Functionalized Tips. *Phys. Rev. B* **2014**, *90*, 085421.

(29) Majzik, Z.; Pavliček, N.; Vilas-Varela, M.; Pérez, D.; Moll, N.; Guitián, E.; Meyer, G.; Peña, D.; Gross, L. Studying an Antiaromatic Polycyclic Hydrocarbon Adsorbed on Different Surfaces. *Nature Commun.* **2018**, *9*, 1198.

(30) This level of calculations has been found to reproduced quantitatively key electronic properties of other PAHs, for instance: (a) Cortizo-Lacalle, D.; Mora-Fuentes, J. P.; Strutynski, K.; Saeki, A.; Melle-Franco, M.; Mateo-Alonso, A. Monodisperse N-Doped Graphene Nanoribbons Reaching 7.7 Nanometers in Length. *Angew. Chem. Int. Ed.* **2018**, *57,* 703–708. (b) Belén, M. A.; Cortizo-Lacalle, D.; Conzalvez, C.; Olano, M.; Atxabal, A.; Sun, X.; Melle-Franco, M.; Hueso, L. E.; Mateo-Alonso A. An Electron-Conducting Pyrene-Fused Phenazinothiadiazole. *Chem. Commun.* **2015**, *51*, 10754–10757.

(31) (a) Clar, E. *The Aromatic Sextet*, **1972**, Wiley, New York. (b) Solá, M.; Forty years of Clar's aromatic π-sextet rule. *Front. Chem.* **2013**, *1*, 22.
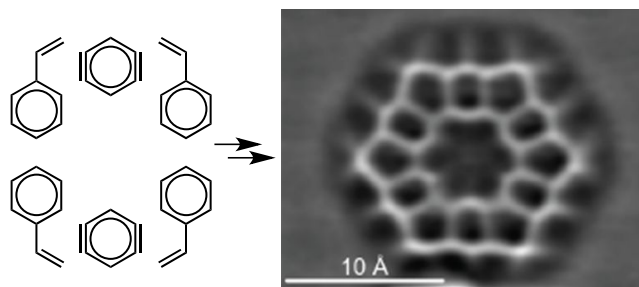
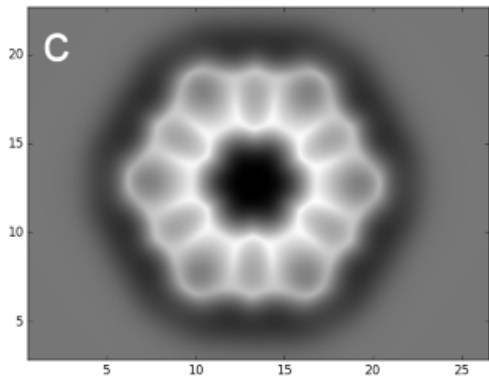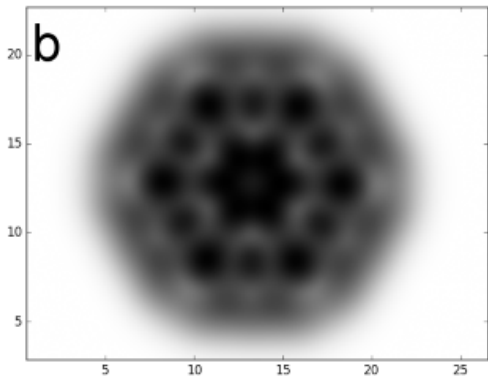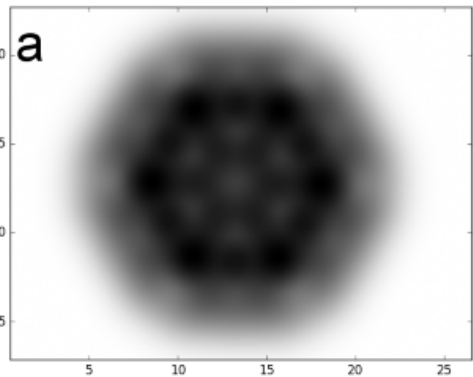(32) Hapala, P.; Temirov, R.; Tautz, S.; Jeníkel, P. Origin of High-

Resolution IETS-STM Images of Organic Molecules with Functionalized Tips *Phys. Rev. Lett.* **2014**, *113*, 226101.

(33) Similar to previous findings: (a) Ellner, M.; Pavliček, N.; Pou, P.; Schuler, B.; Moll, N.; Meyer, G.; Gross, L.: Pérez, R. The Electric Field of CO Tips and Its Relevance for Atomic Force Microscopy. *Nano Lett.* **2016**, *16*, 1974–1980. (b) Hapala, P.; Svec, M.; Stetsovych, O.; Heijden, N. J.; Ondracek, M.; Lit, J.; Mutombo, P.; Swart, I.; Jelínek, P. Mapping the Electrostatic Force Field of Single Molecules from High-Resolution Scanning Probe Images. *Nature Commun.* **2016**, *7*, 11560.

(34) For values of the measured and simulated apparent bond lengths see Supporting Information.

1
2
3
4
5
6
7
8
9
10
11
12
13
14
15
16
17
18
19
20
21
22
23
24
25
26
27
28
29
30
31
32
33
34
35
36
37
38
39
40
41
42
43
44
45
46
47
48
49
50
51
52
53
54
55
56
57
58
59
60

1
2
3
4
5
6
7
8
9
10
11
12
13
14
15
16
17
18
19
20
21
22
23
24
25
26
27
28
29
30
31
32
33
34
35
36
37
38
39
40
41
42
43
44
45
46
47
48
49
50
51
52
53
54
55
56
57
58
59
60

1
2
3
4
5
6
7
8
9
10
11
12
13
14
15
16
17
18
19
20
21
22
23
24
25
26
27
28
29
30
31
32
33
34
35
36
37
38
39
40
41
42
43
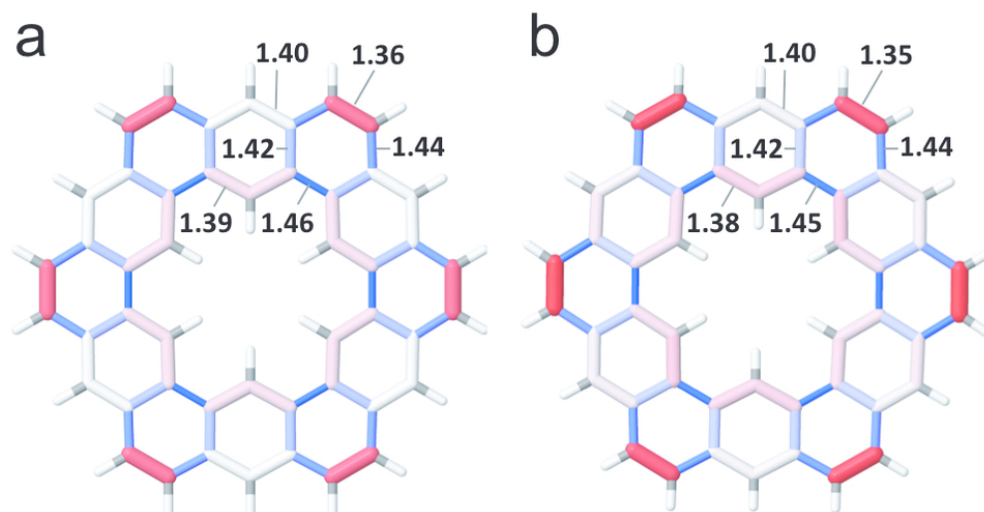44
45
46
47
48
49
50
51
52
53
54
55
56
57
58
59
60

Figure 4. (a) Molecular structure of kekulene (1) computed at the B3LYP-def2-TZVP level in vacuum. (b) Experimental structure from XRD, C2/c space group symmetry. The colors grade with distance from 1.33 Å (red) to 1.40 Å (white) and to 1.47 Å (blue). Bond lengths are in Å

81x43mm (300 x 300 DPI)